Kuldeep; Ahonen, Tommi; Rosenthal, Moritz; Murtomäki, Lasse

Bipolar membrane electrodialysis of Na_2CO_3 and industrial green liquor for producing NaOH: A sustainable solution for pulp and paper industries

Published in:
Chemical Engineering Journal Advances

DOI:
10.1016/j.ceja.2023.100450

Published: 15/05/2023

Document Version
Publisher's PDF, also known as Version of record

Please cite the original version:
Kuldeep, Ahonen, T., Rosenthal, M., & Murtomäki, L. (2023). Bipolar membrane electrodialysis of Na_2CO_3 and industrial green liquor for producing NaOH: A sustainable solution for pulp and paper industries. *Chemical Engineering Journal Advances* , *14*, Article 100450. https://doi.org/10.1016/j.ceja.2023.100450

Chemical Engineering Journal Advances 14 (2023) 100450

Contents lists available at ScienceDirect

Chemical Engineering Journal Advances

journal homepage: www.sciencedirect.com/journal/chemical-engineering-journal-advances

Bipolar membrane electrodialysis of Na_2CO_3 and industrial green liquor for producing NaOH: A sustainable solution for pulp and paper industries

Kuldeep [a,1], Tommi Ahonen [b,1], Moritz Karl Rosenthal [a], Lasse Murtomäki [a,*]

[a] *Department of Chemistry and Materials Science, School of Chemical Engineering, Aalto University, PO Box 1600, 00076 AALTO, Finland*
[b] *Department of Chemistry and Materials Science, Andritz Oy, Tammasaarenkatu 1, 00180 Helsinki, Finland*

ARTICLE INFO

Keywords:
Electrodialysis
Ion-exchange membranes
Waste treatment
H_2S and CO_2 recovery

ABSTRACT

Industrial waste with high salinity cannot be drained into waterways due to tightened environmental regulations. Bipolar membrane electrodialysis (BPED) is getting more attraction not only to treat water flows but also to produce valuable commodities. The BPED technique has various advantages in terms of product purity, control over product concentration, having no by-products, low environmental impact, and low energy consumption. In this short paper, we emphasize a comparative study in two different configurations for the treatment of green liquor (a waste solution of NaOH, Na_2S and Na_2CO_3 from pulp mills) with BPED to produce NaOH. The best results are obtained in a five-compartment setup where the capture of H_2S formed from green liquor is possible, followed by the capture of CO_2. This work also indicates that BPED technology is a sustainable solution to treat carbonate-rich waste, which will facilitate the current need to control greenhouse emissions.

1. Introduction

In pulping, the Kraft process is used to dissolve lignin from wood to yield cellulose fibres for paper and packaging materials [1]. This is done by cooking wood chips in a strong alkali solution (white liquor) at a very high temperature. The solution containing the removed lignin and cooking chemicals (black liquor) is generally boiled in a recovery boiler, ending up in a carbonate-rich ash which then washed with water, turning into a waste solution called green liquor (GL) [2]. The conventional method to recycle GL employs a causticizing reaction with slaked lime ($Ca(OH)_2$) that produces lime-mud ($CaCO_3$) [2]. The recycling of lime-mud requires enormous amounts of energy and produces significant CO_2 emissions. The global pulp and paper market is expected to grow approx. 10% by 2030 due to growing demand in e-commerce and hygiene and personal care products linked to the COVID-19 outbreak [3–4]. Furthermore, the EU aims for a 55% net domestic decrease in greenhouse emissions by 2030 as compared to 1990 [5]. Therefore, new technologies and sustainable solutions to treat GL still need to be investigated.

Luckily, one such sustainable and energy-efficient solution is electrodialysis with bipolar membranes. According to the recent review article by Luo et all, the BPED process is one of the alternatives to capture CO_2 [6]. Iizuka et al. demonstrated a way to capture CO_2 via a 3-step mechanism using BPED technology. They employed NaOH solution to react with CO_2 resulting NaHCO3 solution that was processed via electrodialysis to regenerate NaOH and alkaline carbonate solution, further treated with protons supplied from bipolar membranes (BPM) to recover CO_2 in a recovery cell [7]. The total CO_2 recovery was achieved ca. 40–60% which was further enhanced up to 100% by Valluri et al. by introducing sulfuric acid to the alkaline carbonate compartment [8]. A drastic decrease in pH resulted in CO_2 release in the recovery cell, leading to sodium sulfate solution that can be used as a new feed to a BPED cell to generate NaOH and sulfuric acid [8]. A BPED system in a batch feed and bleed mode in a 5-compartment setup was reported in our previous paper [9]. Pure sodium sulfate and sulfate-rich industrial effluents were used as the feed, and higher than 80% current efficiency and 95% purity of products was achieved [9]. In the same way, using BPED technology, green liquor directly from pulp and paper mills can be efficiently converted into NaOH and alkaline carbonate-rich solution to capture H_2S and CO_2 separately. The major advantage of BPED technology is that valuable chemicals can be easily recovered without any by-products that might impact the environment. Furthermore, recovered chemicals can be reutilized at pulp mills.

Recently, Mandal et al. reported an electrolysis process with cation

---

[*] Corresponding author.
E-mail address: lasse.murtomaki@aalto.fi (L. Murtomäki).
[1] Equal Contribution

https://doi.org/10.1016/j.ceja.2023.100450

exchange membranes where they produced NaOH from pure Na_2CO_3 in two-compartment setups [10]. In two hours, a maximum amount of 0.03 M NaOH was recovered from 0.094 M Na2CO3 at the current density of 3.8 mA cm^{-2} with quite low current efficiency of 53% and high energy consumption of 0.17 kWh mol^{-1}. A similar case study was also carried out by Simon et al. to produce NaOH from Na_2CO_3 and $NaHCO_3$ using membrane electrolysis. A maximum current efficiency of 55 ± 5% was achieved at different current densities, i.e., range 10 to 100 mA cm^{-2} [11]. Iizuka et al. carried out semi-batch BPED of a carbonate-rich solution ($NaHCO_3$) in four-compartment setups where they recovered CO_2 and NaOH in the feed and product compartments [7]. They measured a drastic increase in the current efficiency from 65% to 80% while running the BPED system from 4.8 to 19.2 mA cm^{-2}; the cell stack consisted of 10 or 20 membranes with an area of 210 cm^2 per stack. Similarly, Eswaraswamy et al. performed BPED of green liquor in four-compartment setups at various current densities (range 25–100 mA cm^{-2}) and temperatures (27–50 °C) [12]. The current efficiency of their process decreased after 5 h from 88% to 84% on increasing current density from 25 to 100 mA cm^{-2} due to proton leakage through a CEM.

In this viewpoint, we have carried out BPED of pure Na_2CO_3 and industrial green liquor (effluent composition is listed in Table S1, Supplementary Information) in five-compartment setups. An AEM was added to block the proton transport from the bipolar membrane (BPM) to the main feed compartment, and the results were compared with four compartment setups (without AEM).

2. Experimental and instrumentation

Commercially available membranes (CR61P, AR103P, composed of inert reinforcing fibers and ion-exchange resins) from Suez Water Technologies and Solutions are used in this study; their properties are described in our previous articles [13–14]. The BPM is a sandwich of CR61P and AR103A, treated with Fe(III); it was used as received. All the experiments were carried out using a Micro Flow Cell (Electrocell) with an effective area of 10 cm^2 for both electrodes (Pt-coated titanium) and membranes. Solutions were prepared from 1 M NaOH solution (Merck KGaA, Supelco Titripur, Reag. Ph. Eur.), anhydrous Na_2CO_3 powder (Riedel-de Haën, Reag. ACS) and deionized water.

The performance of BPED was evaluated by measuring concentration change in the product compartment (NaOH) as a function of time in different configurations. The conductivity in the product compartment was continuously monitored and then converted to concentration [15]. All the experiments were conducted at 35 ± 2 °C. The first set of experiments were carried out in a two-compartment configuration with only CEM followed by BCB or BCAB configuration. The BCB configuration contains four compartments, i.e., the cathode, feed and product, and anode compartment, whereas the BCAB configuration contains five compartments. A schematic of BPED configurations is shown in Fig. 1. All experimental parameters including cell configurations, stream concentrations, and current densities used in this study are tabulated in Table S2 of supplementary information.

3. Result and discussion

A two-compartment setup ($+|Na_2CO_3|CEM|NaOH|-$) was firstly investigated at different current densities and electrolyte concentrations to find the suitable condition for BPED treatment of either pure Na_2CO_3 or green liquor. The electrochemical reactions (Eqs. 1 − 3) in this setup are as follows:

At the anode:

$$2CO_3^{2-} + H_2O \rightarrow 2HCO_3^{-} + \frac{1}{2}O_2(\uparrow) + 2e^- \tag{1}$$

At the CEM:

$$Na^+(Na_2CO_3) \rightarrow Na^+(NaOH) \tag{2}$$

At the cathode:

$$2H_2O + 2e^- \rightarrow 2OH^- + H_2(\uparrow) \tag{3}$$

Fig. 2 shows the current efficiency variation with the counter-ion concentration in the two-compartment setup. At a low counter-ion (Na+) concentration on both sides of the CEM, the high current efficiency of 90% was observed that decreased down to 70% on increasing counter-ion concentration at the constant current density of 30 mA cm^{-2}, indicating a selectivity decrease of the membrane. In IEMs, the relation between permselectivity and concentration of the bathing

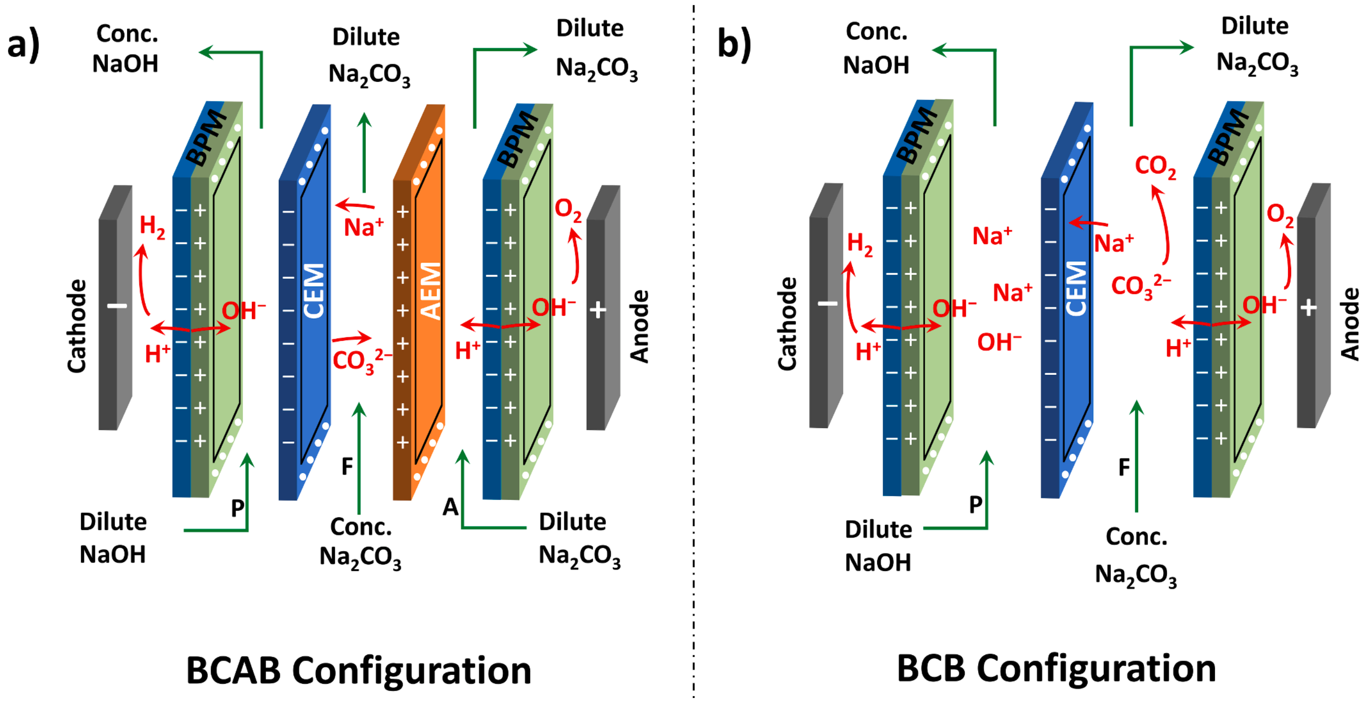

Fig. 1. Schematic of BPED system a) −|BPM-CEM-AEM-BPM|+ or (BCAB), b) −|BPM-CEM-BPM|+ or (BCB) configuration.

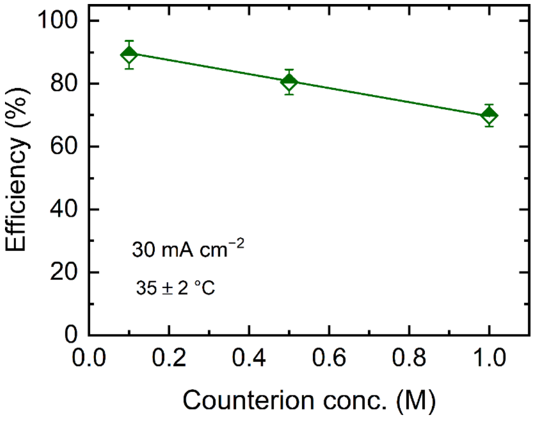

Fig. 2. The current efficiency variation with counter-ion concentration, i.e., Na^+ in a two-compartment setup.

solution can easily be understood with the Donnan equilibrium [16–17], i.e., for 1:1 electrolyte, Eq. (4):

$$c_2^{\mathrm{M}} = -\frac{X}{2} + \sqrt{\left(\frac{X}{2}\right)^2 + \frac{(\gamma_{\pm}^{\mathrm{w}})^2}{\gamma_1^{\mathrm{M}}\gamma_2^{\mathrm{M}}}(c_{12}^{\mathrm{w}})^2} \tag{4}$$

where c_2^{M} is the concentration of co-ion inside the membrane, X is the fixed charge concentration of the membrane, γ is the activity coefficient, and c_{12}^{w} is the concentration of the electrolyte in the bathing aqueous solution. Clearly, from the above equation, increasing bathing solution concentration would lead to a decrease in the permselectivity of the membrane and eventually the current efficiency of the electrodialysis process. Furthermore, at a low solution concentration the limiting current is lower, and with the fixed current density the depletion of salts next to the membrane is more pronounced, which may lead to water dissociation [17], also decreasing the current efficiency. However, in our case, spacers were used near the membrane surface and a high circulation rate (50 ml min^{-1}) of the electrolytes that decreases concentration polarization.

In addition, slightly better current efficiency was observed on increasing current density at a fixed counter-ion concentration, Fig. 3. From the theoretical point of view of ideal homogenous IEMs, current efficiency should decrease with increasing current density because of increase in concentration polarization [18]. Also, the definition of the current efficiency hints a decrease with increasing current density (Eq. (5)):

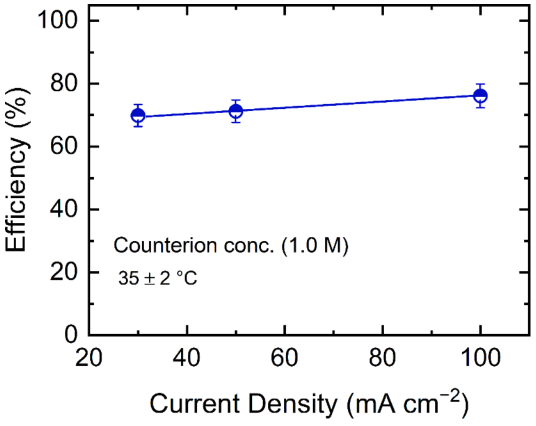

Fig. 3. Current efficiency variation with current density in a two-compartment setup.

$$\eta \propto \frac{J_T}{I} \propto \frac{J_{\mathrm{Diff}} + (J_{\mathrm{mig}} \propto I)}{I} \tag{5}$$

where η is the current efficiency, J_T is a total ionic flux which is the sum of diffusion and migration flux, and I is the current density. However, increasing current efficiency with increased current density has been explained via the inhomogeneity of the membrane, i.e., its uneven distribution of the fixed charged groups [19–21].

For practical operation, we conducted these experiments at the reasonable concentration of the bathing solution, i.e., 1 M on both sides of the membrane. A noticeably ca. 8% higher current efficiency is observed at 100 mA cm^{-2} than at 30 mA cm^{-2}. Therefore, the current density of 100 mA cm^{-2} is selected for GL-BPED operations. If the experiments were run at lower concentrations, the current efficiency would be higher than in Fig. 3 but the effect of current density would be rather small [22].

Fig. 4 shows an experimentally observed trend in the product concentration (NaOH) stream during BPED of pure Na_2CO_3 and 50% diluted Green Liquor (GL). Clearly, a five-compartment experiment with BCAB configurations showed better performance in terms of product concentration than four-compartment experiments, i.e., BCB configuration. It is because the AEM in BCAB configuration excludes protons formed in the BPM, whereas in the absence of AEM, i.e., in the BCB configuration, the feed stream receives protons that can easily migrate through the CEM to the product flow (NaOH), neutralizing hydroxide ions. We have captured this phenomenon by pH measurement of the feed solutions, Fig. 5.

A decrease in pH of the feed in BCB run was observed due to continuous influx of protons from BPM. In contrast, a slightly increased or constant pH of the feed in BCAB run was noticed, which was possibly due to hydroxyl ions leakage through CEM. Furthermore, gas evolution from feed streams (possibly CO_2 in the case of pure Na2CO3 and a possible mixture of CO_2 and H_2S in GL) was also detected in the BCB configuration, confirming the interference of protons in the feed. In contrast, no gas bubbles in the feed compartment were seen in the BCAB configuration as high pH prevented CO_2 release. Yet, release of gas in BPED of GL was observed in the solution (say, solution 'A') between the AEM and the BPM (Fig. 1) where pH was dropped significantly due to transfer of protons from the BPM.

Surprisingly, pH of solution 'A' remains higher than 7.3 throughout the time frame of the experiments, which indicates that the gas was only H_2S. A possible mechanism of the partial release of H_2S follows the following mechanism, Eqs. (6 – 8):

$$S^{2-} + H^+ \leftrightarrow SH^- \tag{6}$$

$$CO_3^{2-} + H^+ \leftrightarrow HCO_3^- \tag{7}$$

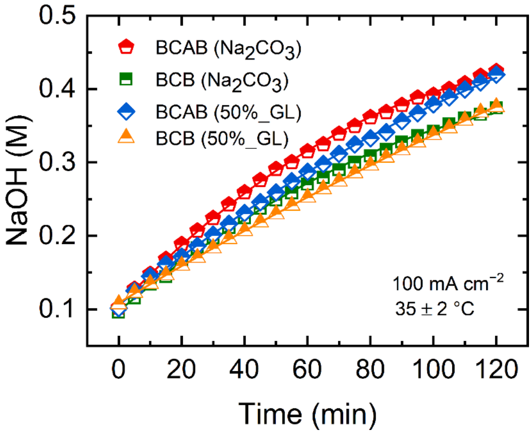

Fig. 4. Product concentration (NaOH) variation with time.

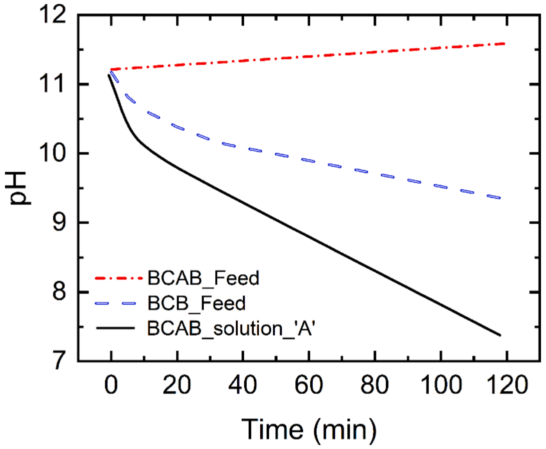

Fig. 5. pH study of feeds (Na2CO3) in different configuration of BPED and solution ‘A’.

$$HCO_3^- + SH^- \leftrightarrow CO_3^{2-} + H_2S(\uparrow) \quad (8)$$

This is confirmed by in-house tracking of CO_2 by 990 micro-GC instruments in BPED of pure Na_2CO_3 in the BCAB configuration. The results showed that no CO_2 was released from solution ‘A’ in BCAB configuration (Figure S1, Supplementary Information) in the same time frame of earlier experiments.

A long run of BPED with undiluted and 50% diluted GL was also carried out in both configurations (Supplementary Information), which provided new, unexpected results. In the BCB configuration, precipitation of elemental sulfur (crystalline S_8) was observed (see X-ray diffraction data in Figure S3 of Supplementary Information) in the anodic compartment as well on the surface of the anode, along with the decrease in pH from 12 to 3. This was due to leakage of SH^- through the cationic layer of the BPM, forming polysulfides (H_2S_n) that eventually decomposed to elemental sulfur via releasing protons in the anodic compartment. The mechanism of elemental sulfur formation from SH^- at the anode is described elsewhere [23–24]. Yet, no deformation or decoloration in AR103A of BPM (close to the anode) was observed. Furthermore, in long-run experiments, all ionic species were depleted from the feed, resulting in final conductivity of 0.43 mS cm^{-1} which caused a large ohmic loss in the system. In contrast, in the BCAB configuration, no elemental sulfur precipitate or pH change was observed in the anodic compartment during the operation. This can be explained by the Donnan failure (selectivity failure) inside the membranes. As shown in Eq. (4), the membrane selectivity decreases at high electrolyte concentrations which was also proved when concentrated electrolytes (Figure S4, Supplementary Information), either 50% diluted or undiluted GL, was fed near the BPM surface in the BCB configuration. In this case, the cation selective part of the BPM lost its selectivity and SH− ions would be transferred to the anode, whereas they would be prevented by an AEM between the BPM and feed. Yet, a bright yellow solution between AEM and BPM was observed after the long run. The actual reason for this yellow colour is unknown but it might be due to dissolved colloidal sulfur. The yellow solution was turned white upon heating, indicating the release of a volatile gas (H2S) leaving behind a solid precipitate (amorphous) mixture of Na_2CO_3 and $Na_2C_2O_4$ as confirmed with XRD (Supplementary Information, Figure S3). Furthermore, dynamic light scattering measurement showed particles of 3000 – 4000 nm (Z-average) for 50% diluted GL and 3000 – 7000 nm for undiluted GL (see Figure S5, Supplementary information).

4. Conclusions

Our results provide insights into the usability of BPED treatment of GL from pulp mills. The best results were achieved in the BCAB configuration where higher product concentration was achieved than in the BCB configuration. In addition, elemental sulfur formation in BCB configuration can be an issue in the scalability of BPED operation for GL from pulp mills. Yet, future research would confirm whether elemental sulfur formation can be avoided by diluting the green liquor, or if a higher process efficiency can be reached with dilution. Furthermore, concentrated GL may contain dissolved sulfur particles that would block membrane pores and eventually cause fouling or scaling of membranes. Our studies with BCAB configuration showed a possible method for the removal of H_2S from an alkaline carbonate solution that can be further treated for CO_2 capture. The BPED of GL with the BCAB configuration followed by the CO_2 capture might be a sustainable solution for a successful treatment. The comparative studies in BCAB and BCB configuration add significant understanding of the BPED technology.

Declaration of Competing Interest

The authors declare no conflict of interest.

Data availability

Data will be made available on request.

Supplementary materials

Supplementary material associated with this article can be found, in the online version, at doi:10.1016/j.ceja.2023.100450.

References

[1] M.H. Lahtinen, J. Mikkilä, K.S. Mikkonen, I. Kilpeläinen, J. Agric. Food Chem. 69 (21) (2021) 5955–5965. https://pubs.acs.org/doi/10.1021/acs.jafc.1c00705.
[2] F.M. Martins, J.M. Martins, L.C. Ferracin, C.J. da Cunha, J. Hazard. Mater. 147 (1–2) (2007) 610–617. https://www.sciencedirect.com/science/article/pii/S0304389407001215.
[3] I. Tiseo, Global market size of paper and pulp 2021-2029, (https://www.statista.com/statistics/1073451/global-market-value-pulp-and-paper/).
[4] Pulp and paper market size, growth, trends, report 2022-2030 (https://www.globenewswire.com/news-release/2022/07/21/2484132/0/en/Pulp-and-Paper-Market-Size-to-Worth-Around-USD-380-12-Bn-by-2030.html).
[5] 5 facts about the EU’s goal of climate neutrality (https://www.consilium.europa.eu/en/5-facts-eu-climate-neutrality/).
[6] Y. Luo, Y. Liu, J. Shen, B.V. der Bruggen, Membranes 12 (9) (2022) 829, https://doi.org/10.3390/membranes12090829.
[7] A. Iizuka, K. Hashimoto, H. Nagasawa, K. Kumagai, Y. Yanagisawa, A. Yamasaki, Sep. Purif. Technol. 101 (2012) 49–59, https://doi.org/10.1016/j.seppur.2012.09.016.
[8] S. Valluri, S.K. Kawatra, Fuel Process. Technol. 213 (2021), 106691, https://doi.org/10.1016/j.fuproc.2020.106691.
[9] Kuldeep, W.D. Badenhorst, P. Kauranen, H. Pajari, R. Ruismäki, P. Mannela, L. Murtomäki, Membranes 11 (9) (2021) 718, doi:10.3390/membranes11090718.
[10] P. Mandal, B. Eswaraswamy, P. Goel, K.S. Kumar, S. Chattopadhyay, Sep. Purif. Technol. 262 (2021), 118347, https://doi.org/10.1016/j.seppur.2021.118347.
[11] A. Simon, T. Fujioka, W.E. Price, L.D. Nghiem, Sep. Purif. Technol. 127 (2014) 70–76, https://doi.org/10.1016/j.seppur.2014.02.020.
[12] B. Eswaraswamy, P. Mandal, P. Goel, A. Chandra, S. Chattopadhyay, J. Environ. Chem. Eng. 10 (3) (2022), 107628, https://doi.org/10.1016/j.jece.2022.107628.
[13] Kuldeep, P. Kauranen, H. Pajari, R. Pajarre, L. Murtomäki, Chem. Eng. J. Adv. 8 (2021) 100169, doi:10.1016/j.ceja.2021.100169.
[14] Kuldeep, J.A. Manzanares,P. Kauranen, S. Mousavihashemi, L. Murtomäki, ChemElectroChem 9 (11) (2022) e202200403, doi:10.1002/celc.202200403.
[15] R.C. Weast, Handbook of Chemistry and physics: A ready-Reference Book of Chemical and Physical Data, 56th ed., CRC Press, Cleveland, 1975.
[16] T. Luo, S. Abdu, M. Wessling, J. Mem. Sci. 555 (2018) 429–454, https://doi.org/10.1016/j.memsci.2018.03.051.
[17] T. Aritomi, T. van den Boomgaard, H. Strathmann, Desalination 104 (1–2) (1996) 13–18, https://doi.org/10.1016/0011-9164(96)00021-5.
[18] K. Kontturi, L. Murtomäki, J.A. Manzanares, Ionic Transport Processes in Electrochemistry and Membrane Science, Oxford University Press, Oxford, 2015.
[19] S. Mafé, J.A. Manzanares, M.J. Hernández, J. Pellicer, J. Colloid Interface Sci. 145 (2) (1991) 433–440, https://doi.org/10.1016/0021-9797(91)90374-H.
[20] J.A. Manzanares, S. Mafé, J. Pellicer, J. Chem. Soc. Faraday Trans. 88 (16) (1992) 2355–2364, https://doi.org/10.1039/FT9928802355.
[21] A.V. Sokirko, J.A. Manzanares, J. Pellicer, J. Colloid Interface Sci. 168 (1994) 32–39, https://doi.org/10.1006/jcis.1994.1390.

[22] Y. Tanaka, J. Mem. Sci. 266 (1–2) (2005) 6–17, https://doi.org/10.1016/j.memsci.2005.05.005.

[23] Z. Mao, A. Anani, R.E. White, S. Srinivasan, A.J. Appleby, J. Electrochem. Soc. 138 (1991) 1299–1303. https://iopscience.iop.org/article/10.1149/1.2085775.

[24] E. Ntagia, E. Fiset, L.T.C. Hong, E. Vaiopoulou, K. Rabaey, J. Hazard. Mater. 388 (2020), 121770, https://doi.org/10.1016/j.jhazmat.2019.121770.